Supplementary material

Hydroxyl-functionalized covalent organic framework enables high-affinity adsorption of myricetin

Shuangyu Wei, Xin Peng, Lu Bai, Wei Wei, Feiyue Zhang, Chaoqun You* and Fei Wang*

Jiangsu Co-Innovation Centre of Efficient Processing and Utilization of Forest Resources, Jiangsu Key Lab for the Chemistry and Utilization of Agro-Forest Biomass, College of Chemical Engineering, Nanjing Forestry University, Nanjing 210037, PR China

Corresponding authors:

Fei Wang, E-mail address: hgwf@njfu.edu.cn

Chaoqun You, E-mail address: chemyoucq@njfu.edu.cn

Number of pages: 17

Tables:7

Figures: 12

Contents

Table S4 Kinetic models parameters for adsorption of myricetin on COFs.

Table S5 Isotherm models parameters for adsorption of myricetin on COFs

Table S6 Thermodynamic parameters of myricetin adsorption on COFs.

Table S7 Comparison of the equilibrium time and qm of myricetin onto COFs with some other materials

3. References

1. Experimental section

1.1 Materials

All available starting compounds and solvents, unless otherwise noted, were obtained from J&K scientific LTD. myricetin (≥97 %), rutin (≥98 %) were purchased from Shanghai Macklin Biochemical Co. quercetin (≥97 %), kaempferol (95 %) were purchased from Shanghai Yuanye Bio-Technology Co. luteolin (>97 %) were purchased from Shanghai Bide Pharmaceutical Technology Co.

1.2 Instruments

Solid- state ^{13}C NMR spectra were recorded on an AVIII 500 MHz solid-state NMR spectrometer. X-ray photoelectron spectroscopy (XPS) measurements were conducted on a R3000/VUV5K/ MX-650 XPS/UPS system, the take-off angle of the photoelectron was fixed at 90° with respect to the sample plane. Fourier transform infrared (FT-IR) spectra (KBr pellets) were obtained using a SHIMADZU IRAffinity^{-1} spectrophotometer. Thermogravimetric analysis (TGA) was recorded on a SHIMADZU DTG-60 thermal analyzer under N_2. The operational range of the instrument was from 50 °C to 800 °C at a heating rate of 5 °C min^{-1} with N_2 flow rate of 30 mL min^{-1}. Powder X-ray diffraction (PXRD) data were collected on a PANalytical B.V. Empyrean diffractometer using Cu Kα radiation (λ = 1.5418 Å) over the 2θ range of 2.0-40.0° with a step size of 0.02° and a counting time of 2 s per step. The sorption isotherm for N_2 was measured by using a Quantachrome Autosorb-IQ analyzer with ultra-high-purity gas (99.999% purity). To assess pore size distributions for DHBD-COF, DHA-COF and PA-COF, nonlocal density functional theory (NLDFT) was adopted to analyze the N_2 isotherm on the basis of the model of N_2@77 K on carbon with slit pores and the method of non-negative regularization. For scanning electron microscopy (SEM) image, JEOL JSM-6700 scanning electron microscope was applied. Transmission electron microscopy (TEM) image was obtained on JEM-2100 transmission electron microscopy. UV—vis transmittance and absorption spectra were recorded on a UV-2700 Spectrophotometer (Shimadzu).

1.3 *Synthesis of DHBD-COF*

DHBD (0.06 mmol, 14.17 mg) and TAPT (0.04 mmol, 14.53 mg) were weighed and added into a Pyrex tube. Subsequently, 1 mL of mesitylene and 0.1 mL of acetic acid (6 M) were introduced as the solvent system. After thorough mixing, the tube was quickly frozen in a liquid nitrogen bath, evacuated, and flame-sealed. The sealed tube was then heated at 120 °C for 3 days. After the reaction, the solid product was collected by filtration and washed thoroughly with acetone. Finally, the obtained material was dried under vacuum at 60 °C to afford DHBD-COF.

1.4 *Synthesis of DHA-COF*

DHA (0.066 mmol, 10.96 mg) and TAPT (0.044 mmol, 15.59 mg) were weighed and added into a Pyrex tube. Subsequently, 0.5 mL of mesitylene, 0.5 mL of dioxane, and 0.1 mL of acetic acid (3 M) were introduced as the solvent system. After thorough mixing, the tube was quickly frozen in a liquid nitrogen bath, evacuated, and flame-sealed. The sealed tube was then heated at 120 °C for 3 days. After the reaction, the solid product was collected by filtration and washed thoroughly with acetone. Finally, the obtained material was dried under vacuum at 60 °C to afford DHA-COF.

1.5 *Synthesis of PA-COF*

PA (0.066 mmol, 8.85 mg) and TAPT (0.044 mmol, 15.59 mg) were weighed and added into a Pyrex tube. Subsequently, 0.5 mL of mesitylene, 0.5 mL of dioxane, and 0.1 mL of acetic acid (6 M) were introduced as the solvent system. After thorough mixing, the tube was quickly frozen in a liquid nitrogen bath, evacuated, and flame-sealed. The sealed tube was then heated at 80 °C for 3 days. After the reaction, the solid product was collected by filtration and washed thoroughly with acetone. Finally, the obtained material was dried under vacuum at 60 °C to afford PA-COF.

1.6 Adsorption experiments

The adsorption properties of the COFs we synthesized were evaluated through a series of adsorption tests. Standard flavonoid compounds of myricetin, quercetin, luteolin, kaempferol, and rutin (Fig. S1) were dissolved in methanol to prepare stock solutions. The stock solutions were then diluted to prepare working solutions with different concentrations. To investigate the adsorption kinetics, 4 mg of COF was placed in a 10 mL centrifuge tube containing 10 mL of the flavonoid working solution (100 mg/L). The mixtures were shaken in a constant-temperature shaker at 150 rpm for 0-120 minutes. Adsorption isotherm experiments were conducted at three temperatures—298 K, 308 K, and 318 K. Flavonoid working solutions with concentrations ranging from 25 to 250 mg/L were prepared. 10 mL of flavonoid solutions with varying concentrations were placed into 10 mL centrifuge tubes, after which 4 mg of the COF adsorbent was introduced. The mixtures were placed in a thermostatic shaker for 3 hours to ensure adequate adsorption. The supernatant was filtered using a 0.22 μm membrane, and the resulting solution was analyzed via UV–vis spectrophotometry. The adsorption capacity was calculated using Eq. (1)：

$$q_t = (C_O - C_t)V/m\#（1）$$

Where q_t (mg/g) is the adsorption capacity, C_0 (mg/L) is the initial concentration of flavonoids, C_t (mg/L) is the concentration of flavonoid compounds in the supernatant after adsorption, V (L) is the volume of the flavonoids solution, m (mg) is the mass of the adsorbent.

1.7 Adsorption kinetics and isotherms

In order to study the adsorption kinetics, pseudo-first-order models (Eq. (2)) and pseudo-second-order models (Eq. (3)) were applied to fit and analyze the experimental data. These models are commonly used to describe the adsorption of a solute from a liquid solution onto a solid adsorbent.

$$\ln(q_e - q_t) = \ln q_e - k_1 t\#（2）$$

$$t/q_t = 1/k_2 q_e^2 + t/q_e \#（3）$$

where q_e is the equilibrium adsorption capacity, q_t is the adsorption capacity at time t. k_1 (1/min) and k_2 (g/mg/min)) are the adsorption rate parameters of pseudo-first-order and pseudo-second-order kinetic models, respectively.

To investigate the adsorption isotherms, the Langmuir (Eq. (5)) and Freundlich (Eq. (6)) models were employed, according to the following equations:

$$q_e = Q_m K_L C_e / 1 + K_L C_e \#(4)$$

$$ln q_e = (1/n) ln C_e + ln K_F \#(5)$$

Where q_e and q_m represent the equilibrium adsorption capacity and the maximum adsorption capacity, respectively. C_e (mg/L) is the equilibrium concentration. K_L (L/mg) and K_F (mg/g(L/mg)$^{1/n}$) are constants of the Langmuir and Freundlich isotherm models, respectively, related to the adsorption energy and representing the adsorption capacity, while 1/n is the Freundlich isotherm constant.

2. Results and Discussions

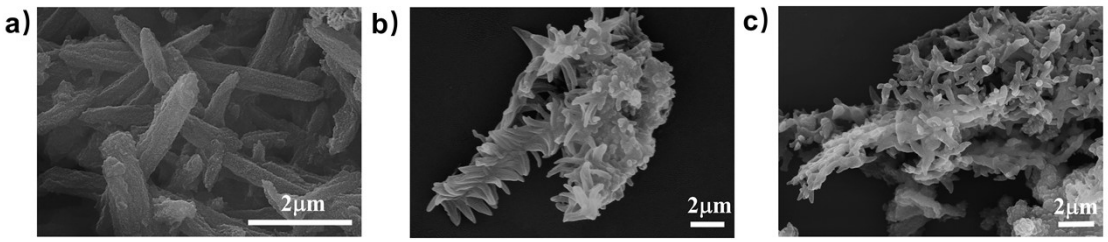

Fig. S1 SEM images of (a) DHBD-COF, (b) DHA-COF and (c) PA-COF.

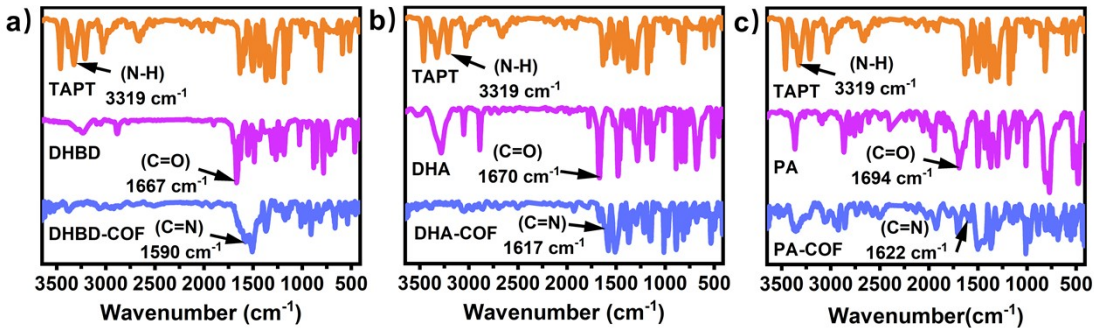

Fig. S2 FT-IR spectra of (a) DHBD-COF, (b) DHA-COF and (c) PA-COF.

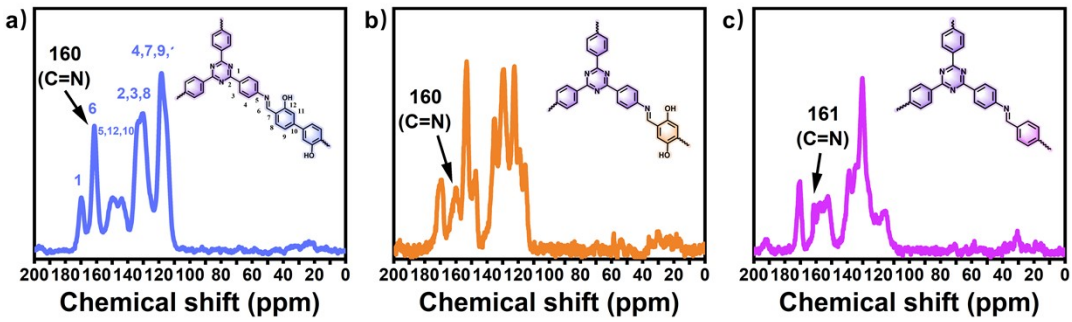

Fig. S3 Solid state ^{13}C NMR of (a) DHBD-COF,(b) DHA-COF, and (c) PA-COF.

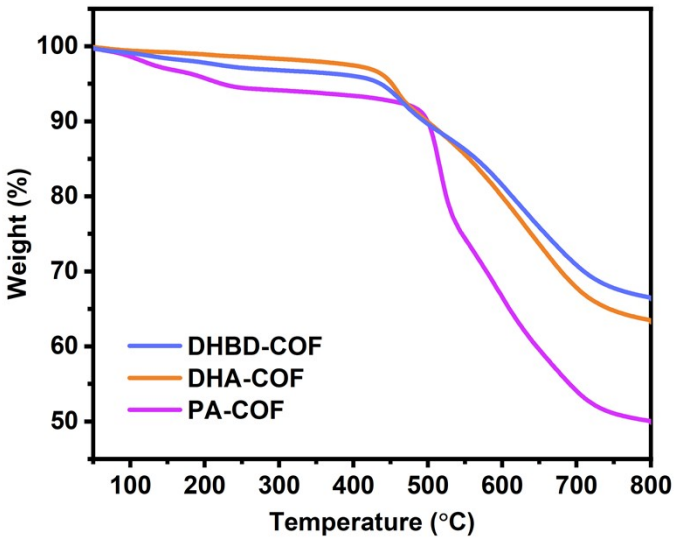

181 **Fig. S4** TGA curve of DHBD-COF、DHA-COF and PA-COF.

182

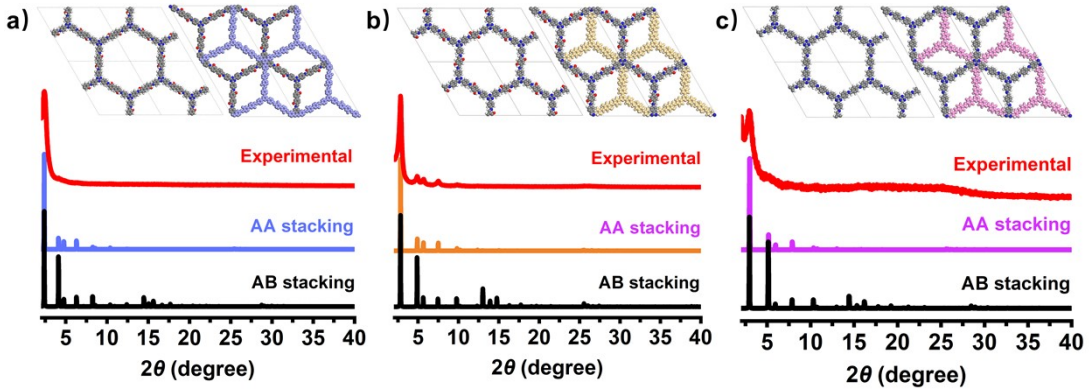

183 **Fig. S5** PXRD patterns of (a) DHBD-COF, (b) DHA-CPF, (c) PA-COF-AA and AB stacked

184 simulated.

185

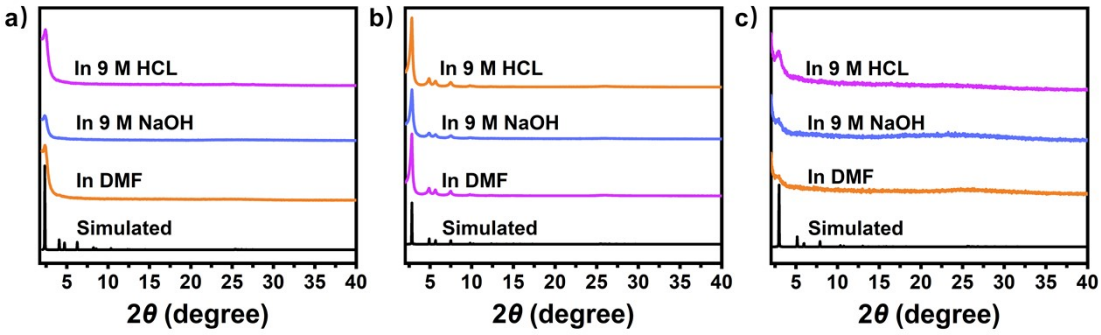

Fig. S6 PXRD patterns of (a) DHBD-COF, (b) DHA-COF, and (c) PA-COF after treatment with HCl (9 M), NaOH (9 M), and DMF.

186

187

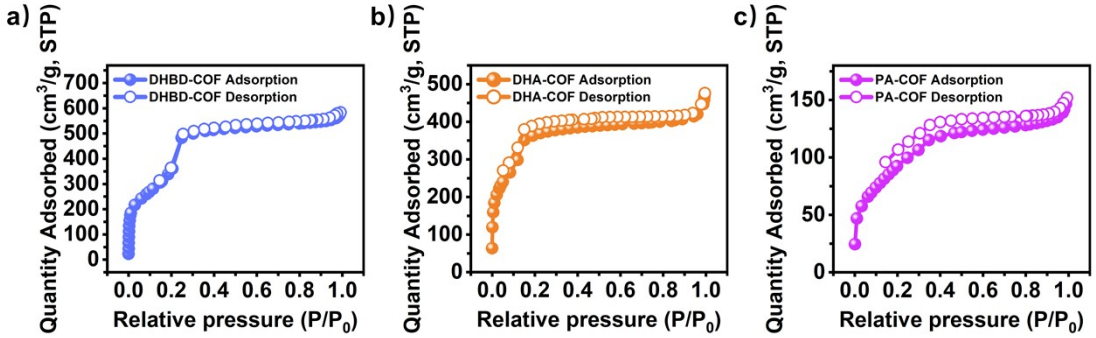

Fig. S7 N_2 adsorption-desorption isotherms at 77 K for (a) DHBD-COF, (b) DHA-COF and (c) PA-COF.

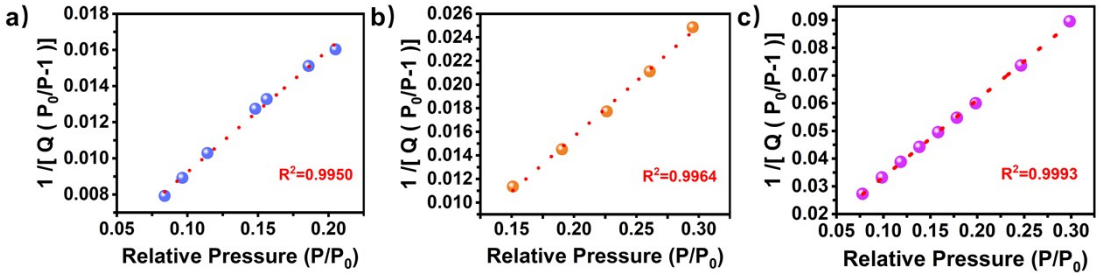

Fig. S8 BET plot of (a) DHBD, (b) DHA-COF and (c) PA-COF calculated from N_2 adsorption isotherm at 77 K.

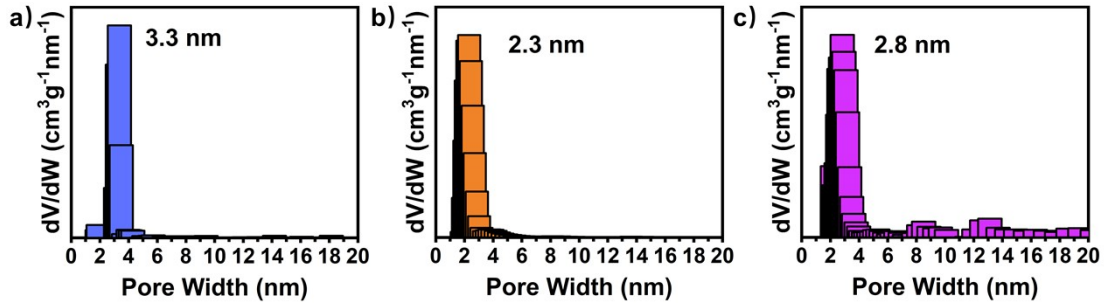

Fig. S9 Pore size distribution for (a) DHBD-COF, (b) DHA-COF and (c) PA-COF.

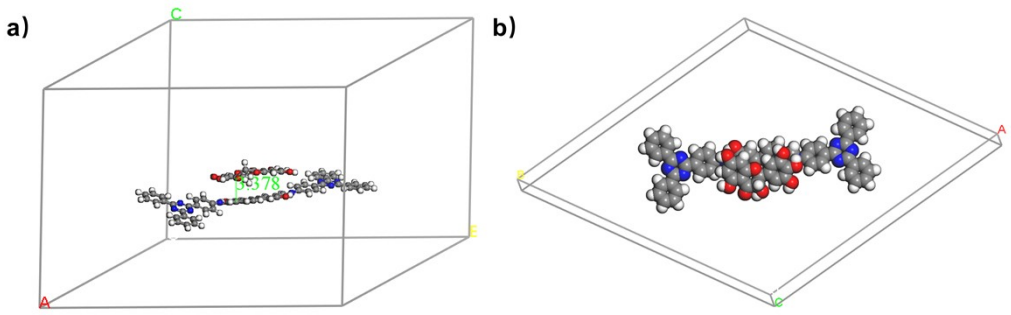

197 **Fig. S10** The front view (a) and top view (b) of the DHBD-COF after adsorbing
198 myricetin were simulated by Materials Studio.
199

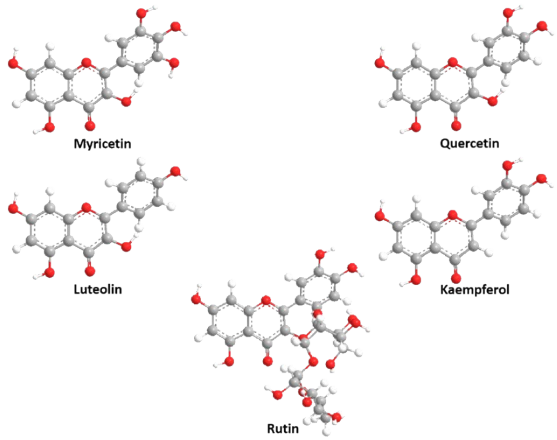

200 **Fig. S11** Structure of myricetin, quercetin, luteolin, kaempferol and rutin. gray: carbon red: oxygen
201 White: hydrogen.
202

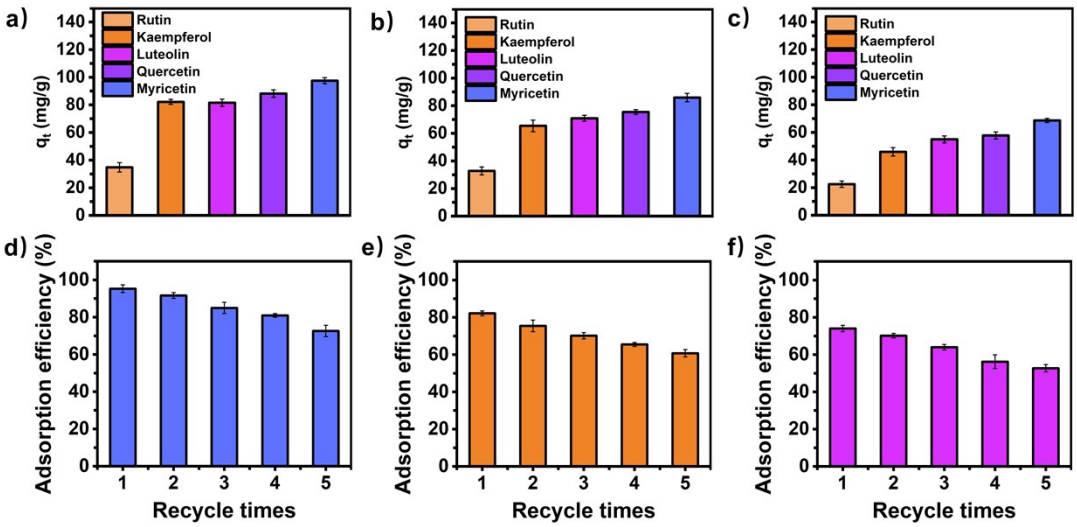

203 **Fig. S12** Comparison of the adsorption performance of five flavonoids by (a) DHBD-COF, (b)
204 DHA-COF and (c) PA-COF. Regeneration performance of (d) DHBD-COF、(e) DHA-COF and
205 (f) PA-COF for myricetin.

Table S1 Unit cell parameters and fractional atomic coordinates for DHBD-COF calculated based on the AA stacking ***hcb*** net.

Space group	P6		
Measured unit cell	a = b = 43.2437 Å, c = 3.5083 Å, α = β = 90°, γ = 120°		
Pawley refinement	R_p = 3.58%, R_{wp} = 5.12%		
atoms	x	y	z
N1	-0.63174	0.68659	4.01158
C2	-0.64027	0.59915	4.01158
C3	-0.61973	0.5837	4.01158
C4	-0.58351	0.60422	4.01158
C5	-0.56824	0.64023	4.01158
C6	-0.58881	0.65568	4.01158
C7	-0.62497	0.63527	4.01158
C8	-0.57363	0.55613	4.01158
N9	-0.56171	0.58921	4.01158
C10	-0.56667	0.50504	4.01158
C11	-0.54678	0.48889	4.01158
C12	-0.51056	0.50856	4.01158
C13	-0.49469	0.54475	4.01158
C14	-0.51442	0.56111	4.01158
C15	-0.55086	0.54109	4.01158
C16	-0.29822	0.35336	4.01158
O17	-0.49771	0.59647	4.01158
H18	-0.66966	0.58238	4.01158
H19	-0.63234	0.55431	4.01158
H20	-0.53887	0.65715	4.01158
H21	-0.5762	0.68507	4.01158
H22	-0.60291	0.53849	4.01158
H23	-0.59611	0.48879	4.01158
H24	-0.55997	0.45946	4.01158
H25	-0.46527	0.56126	4.01158
H26	-0.51478	0.60525	4.13862

Table S2 Unit cell parameters and fractional atomic coordinates for DHA-COF calculated based on the AA stacking ***hcb*** net.

Space group	P6		
Measured unit cell	a = b = 36.2103 Å, c = 3.4040 Å, α = β = 90°, γ = 120°		
Pawley refinement	R_p = 4.29%, R_{wp} = 5.71%		
atoms	x	y	z
C1	0.35249	0.70858	1.47067
N2	0.37492	0.68925	1.47067
C3	0.36148	0.58351	1.47065
C4	0.38477	0.56384	1.47066
C5	0.4281	0.58711	1.47068
C6	0.44729	0.63009	1.4707
C7	0.42404	0.64977	1.47069
C8	0.38082	0.6267	1.47067
C9	0.44225	0.52994	1.47072
N10	0.45392	0.56889	1.47069
C11	0.45762	0.47304	1.47072
C12	0.48449	0.45717	1.47072
C13	0.52743	0.48441	1.47072
O14	0.46864	0.41458	1.47072
H15	0.32825	0.56478	1.47063
H16	0.36842	0.53064	1.47064
H17	0.48055	0.64845	1.47071
H18	0.44001	0.68308	1.47071
H19	0.40999	0.50691	1.47074
H20	0.42471	0.45193	1.47072
H21	0.43747	0.39787	1.47072

Table S3 Unit cell parameters and fractional atomic coordinates for PA-COF calculated based on the AA stacking ***hcb*** net.

Space group	P6		
Measured unit cell	a = b = 34.2 Å, c = 3.4813 Å, α = β = 90°, γ = 120°		
Pawley refinement	R_p = 3.76%, R_{wp} = 5.20%		
atoms	x	y	z
C1	-0.65288	-0.42665	1
C2	-0.63409	-0.45105	1
C3	-0.54295	-0.51686	1
C4	-0.64285	-0.29135	1
N5	-0.62499	-0.3153	1
C6	-0.59102	-0.43274	1
C7	-0.62864	-0.38316	1
C8	-0.53373	-0.44542	1
N9	-0.57324	-0.45906	1
C10	-0.4831	-0.52632	1
C11	-0.56658	-0.38933	1
C12	-0.58523	-0.36479	1
C13	-0.52611	-0.54299	1
H14	-0.68634	-0.44169	1
H15	-0.65295	-0.48444	1
H16	-0.57625	-0.53017	1
H17	-0.53319	-0.37448	1
H18	-0.56577	-0.33142	1
H19	-0.54658	-0.57622	1

Table S4 Kinetic models parameters for adsorption of myricetin on COFs.

	pseudo-first-order			pseudo-second-order		
	R^2	q_e (mg/g)	k_1 (1/min)	R^2	q_e (mg/g)	k_2 (g/mg/min)
DHBD-COF	0.9490	93.98	0.09	0.9834	104.18	0.0011
DHA-COF	0.9814	83.92	0.08	0.9980	93.44	0.0012
PA-COF	0.9714	65.92	0.09	0.9893	73.77	0.0015

Table S5 Isotherm models parameters for adsorption of myricetin on COFs.

		Langmuir			Freundlich		
	T(K)	K_L (L/mg)	Q_m (mg g^{-1})	R^2	K_F (mg/g(L/mg)$^{1/n}$)	n	R^2
DHBD-COF	298	0.14	117.99	0.9966	41.08	4.70315	0.9832
	308	0.095	115.89	0.9803	33.34	4.07386	0.9890
	318	0.048	109.59	0.9899	20.51	3.15963	0.9808
DHA-COF	298	0.083	100.32	0.9678	29.92	4.3158	0.9286
	308	0.058	92.98	0.9970	21.31	3.58924	0.9833
	318	0.035	86.81	0.9954	13.78	2.97913	0.9650
PA-COF	298	0.080	78.12	0.9982	23.31	4.32684	0.9918
	308	0.057	69.99	0.9994	17.13	3.80357	0.9901
	318	0.029	79.75	0.9954	10.79	2.77222	0.9681

Table S6 Thermodynamic parameters of myricetin adsorption on COFs.

	T (K)	ΔG (kJ/mol)	ΔH (kJ/mol)	ΔS (J/K·mol)
DHBD-COF	298	-26.51	-29.26	-9.22
	308	-26.41		
	318	-25.49		
DHA-COF	298	-25.22	-26.94	-5.76
	308	-25.17		
	318	-24.65		
PA-COF	298	-25.13	-25.86	-2.45
	308	-25.11		
	318	-24.18		

Table S7 Comparison of the equilibrium time and q_m of myricetin on COFs with some other materials

Materials	q_m(mg/g)	Ref.
DHBD-COF	117.99	this
DHA-COF	100.32	this
PA-COF	78.12	this
Fe_3O_4–NH2@MIP	19.96	34
$TSNP_{240}$	103.13	35
TzDa-PBA	84.5	36
MPM-MR	81.6	37
COF-TD	124.6	38